Infrared (ATR) Study of Hydrogen Bonding in Solutions Containing Water and Ethylene Carbonate

Paula A. Brooksby and W. Ronald Fawcett*

Department of Chemistry, University of California, Davis, California 95616

Received: February 11, 2000; In Final Form: June 5, 2000

The structure and hydrogen bonding of water in solutions containing EC at different concentrations were examined using infrared (ATR) spectroscopy. Analysis of the OH stretch vibrations of water was performed using several different techniques, and the results were compared to similar analyses found in the literature. Factor analysis and curve fitting show two concentration-dependent regions wherein the structure of water in the mixture is critically disrupted and hydrogen bonding is significantly changed.

1. Introduction

Attenuated total reflection (ATR) spectroscopy is a useful technique for observing the infrared vibrational spectrum of aqueous solutions.[1] The large hydrogen-bond density of liquid water is highly absorbing in the infrared spectrum, and transmission cell techniques require extremely short path lengths in order to avoid saturation effects. For ATR spectroscopy, the effective sample path length (penetration depth of the evanescent wave) is a function of the optical properties of the system, the wavelength, and the angle of incidence of the infrared light. Thus, the path length of the evanescent wave in most typical ATR cells is on the order of microns, which is more suitable for infrared spectroscopy of aqueous solutions or other highly absorbing environments. For this reason, the ATR method is increasingly used to examine the molecular structure of pure water and solutions in which water is a major component.

The mid-infrared and Raman spectrum of liquid water has an intense and broad band envelope at about 3300 cm^{-1} that is assigned to the OH stretching modes.[2−7] Decomposition of the spectral band envelope into Gaussian bands is a common approach that typically gives four adequately resolved bands. The assignment of the four resolved OH stretching bands is described in terms of the individual OH bonds of water representing a single OH oscillator. The two equivalent OH oscillators are coupled, creating the symmetric (ν_1) and asymmetric (ν_3) stretches. For the ν_1 vibration, both oscillator motions are in-phase, whereas the ν_3 vibration represents the out-of-phase motion of the two oscillators. The liquid phase of pure water is further complicated by the competition between inter- and intramolecular OH coupling that promotes delocalization of the OH vibrational mode.[3,6] The delocalized OH mode represents the collective motion of many oscillators, so that the ν_1 and ν_3 stretches are the collective in-phase and out-of-phase vibrations, respectively.

The ν_1 and ν_3 modes typically appear in the infrared spectrum at about 3210 and 3380 cm^{-1}, respectively, and are, in general, assigned to water molecules that are in fully hydrogen-bonded environments. The two additional deconvoluted bands are found at approximately 3530 and 3605 cm^{-1} in the infrared spectrum and are assigned to the vibrations of a partially hydrogen-bonded water molecule. Partially hydrogen-bonded water has one of its OH groups participating in hydrogen bonding to another water molecule, whereas the second OH group is considered as "free" or weakly hydrogen-bonded and appears at the higher value of the two additional deconvoluted band positions given above.

Curve fitting of the water vibrational spectrum into four deconvoluted bands is often used to describe the structure of liquid water by the continuum model.[3−8] This model implies that the pure liquid has an extensive network of hydrogen bonds that produce a continuous distribution of bond angles, bond lengths, and therefore bond energies. The intermolecular interactions that widely distribute the bond lengths and angles also inhomogeneously broaden the stretching vibrational modes.[7] Hence, there is a known[9] correlation between the O···O bond distance in O···H−O bonds and the extent of hydrogen bonding. The band positions and widths of the deconvoluted spectrum provide information regarding this correlation.[9−11]

Despite the complexity of the water vibrational spectrum it is evident that the water stretching modes can be useful for probing the hydrogen-bonding interactions in aqueous solutions. This approach has been widely used to obtain structural information on the hydrophobic and hydrophilic interactions of electrolyte−water solutions for the water isomer HOD[12−15] and to investigate the hydration structure of ether/H_2O,[16−18] crown ether/H_2O,[19,20] amino acid/H_2O,[21,22] and polymer/H_2O mixtures[23−26] to name only a few.

The purpose of this study is to examine the structure of water−ethylene carbonate (EC) solutions using mid-infrared (ATR) spectroscopy for EC concentrations up to 8.1 mol dm^{-3} (mass percent EC = 60). EC is a compound that is important in the rechargeable lithium ion battery industry.[27] Hence, an understanding of the hydration of EC in water will facilitate the examination of water−EC solutions at charged metal interfaces. The hydration of EC is examined by analysis the vibrational spectrum of water in the range from 2700 to 3900 cm^{-1}. Changes in the (curve-fit) vibrational bands of water that accompany a change in the mole fraction of water are used to assess the molecular structure of the solution and the hydrogen-bonding environment.

2. Experimental Procedure

EC (99.7% anhydrous) was purchased from Aldrich and further purified by recrystallization. Nanopure water with a

* To whom correspondence should be addressed. E-mail: fawcett@indigo.ucdavis.edu.

10.1021/jp000551b CCC: $19.00
Published on Web 08/11/2000

resistance higher than 17.9 MΩ was obtained from a Barnstead filtration unit operating with four cartridges for the removal of both organic and ionic impurities. EC and water solutions were prepared using sample weights measured at 24 °C and later converted to molarity. A 20 cm^{-3} pycnometer (calibrated with water at 24 °C) was used to collect a series of seven EC−water solutions with densities ranging from pure water to 60 mass % EC. A linear equation relating the solution density to mass percent of EC was derived and used to convert mass percent of EC to molarity. The best-fit linear equation, eq 1, where ρ is solution density in grams per cubic centimeter and MP is mass percent of EC, was obtained with $R^2 = 0.9994$. The solution density measurements agree well with those of Srivastava et al.[28] (measured at 25 °C).

$$\rho = 0.003085\ \mathrm{MP} + 0.997045 \qquad (1)$$

A Mattson Galaxy 3000 RS-1 spectrometer was used for all infrared measurements. The spectrometer was operated at ambient pressures in an environment that had been purged significantly free of CO_2 and atmospheric water (PUREGAS Air Dryer, model CDA1120). The spectrometer was equipped with a Ge/KBr beam splitter, a mechanical interferometer having cubic mirrors, a water-cooled Globar ceramic source, and an MCT detector. An ATR cell and reflectance accessory (University of California, Davis) was designed to fit into the sample compartment of the Mattson spectrometer and allowed for a ZnSe hemispherical prism (Spectral Systems, 12.7-mm radius) with the planar reflection surface to be mounted horizontally. Solution samples were contained above the prism surface with a glass cell that was held in place by four springs attached at strategic points. A Viton O-ring was placed between the edge of the glass cell wall and the prism with the springs suppling necessary downward pressure to complete the seal. The reflectance accessory was located beneath the ATR cell and consisted of two large planar front-coated gold mirrors. Each mirror was fully adjustable for height, angle, and tilt with respect to the ZnSe prism. The mirror arrangement allowed a range of angle of incidences of the infrared light to be selected and optimally aligned for maximum throughput of radiation. The ATR cell could be reproducibly located above the reflection accessory with a purpose-built holding platform and locator pins. The holding platform was further adjustable for horizontal and vertical movements.

All pATR spectra were obtained using 1 cm^{-1} resolution and calculated by taking the negative logarithm of the ratio of the sample and background single-beam spectra. The empty ATR cell blanketed with argon gas was used to collect the background spectrum. Calibration of the ATR cell was accomplished with a program[29,30] that uses the procedure described by Sperline[31] and Bertie.[32] The pATR spectrum of an optical standard (toluene) for which the refractive indices are tabulated was collected using s- or p-polarized light. Because the ZnSe prism uses only one reflection, the angle of incidence can be determined through a minimization of the sum of the squares of the deviations between the tabulated and measured s- or p-polarized pATR spectra. The angle of incidence was determined to be 41°. Distortions in the sample pATR spectra due to dispersion effects and the dependence of the path length on the frequency were removed by converting the collected pATR spectra to linear absorbance spectra. The "Spectral Conversion Tool" program,[29,30] designed to perform the spectral conversion based on the method of Bertie,[33,34] uses an iterative procedure with the Fresnel equations and the Kramers−Kronig transform. The pATR spectra were converted to the absorbance spectra with a path length of 1.0 μm. Figure 1 illustrates the significance of data correction for the pATR spectrum of pure water following the conversion to an absorbance spectrum.

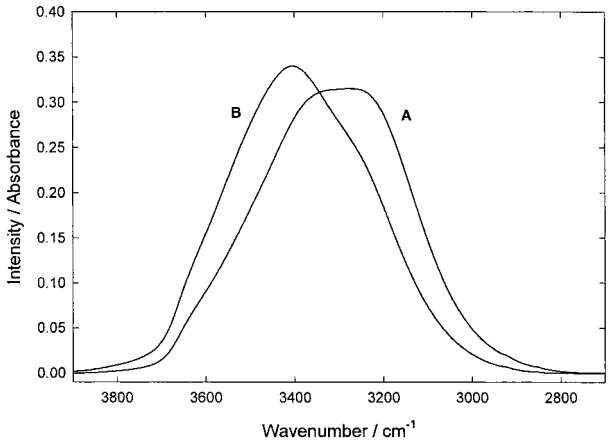

Figure 1. The infrared spectrum of pure water in the range 2700 to 3900 cm^{-1}. (A) Original spectrum collected as pATR and (B) the absorption spectrum following conversion (see text).

LinkFit[35] was used to perform single-dimensional spectral curve fits. Lorentzian, Gaussian, or mixed Lorentzian−Gaussian curves were fit to spectral bands via the Levenberg−Marquardt algorithm. Polynomial baselines can be fit during the nonlinear least squares iteration, or they can be solved for and subtracted from the spectrum prior to curve fitting. Multiple-dimensional curve fits[36] were also performed using a factor analysis routine.[36,37] The pATR spectra collected as a function of known solution concentrations were organized into a matrix, **A**, such that the columns represent the individual pATR spectra and the rows are the pATR values at the wavenumbers used in the analysis. This matrix is factored into two additional matrixes, $\mathbf{A} = \mathbf{BP}$, where the columns of **B** are the basis spectra comprising the pATR spectra in **A**, and the rows, **P**, give the contributions of the basis spectra to the corresponding pATR spectrum. The elements of **P** can be mathematically modeled on the basis of knowledge of the components of the system, stoichiometry, concentrations, pH, and so forth. However, the large sizes of the matrixes created are conveniently simplified by using a numerical analysis routine called singular value decomposition (SVD). SVD factors **A** into smaller matrixes that are more reasonable for transforming the SVD output into **B** and **P**. Furthermore, the SVD output allows the determination of the number of significant basis spectra. If no prior knowledge of the basis spectra is known, then this is an important advantage. The significance of the basis spectra was evaluated numerically by its percent of variance. A basis spectrum was considered insignificant if it accounted for less than 0.01% of the variance. The spectra with percent of variance below 0.01 were attributed to noise and baseline drift. A detailed description of all the software used in this analysis has been published elsewhere.[30]

3. Results

3.1. Factor Analysis of the *ν*OH Bands. Figure 2 shows the infrared spectra from 3900 to 2700 cm^{-1} of water−EC mixtures for a representative range of water-to-EC mole ratios (MRs). The range of compositions studied involved 12 MRs from 333.06 to 3.22 (EC concentrations from 0.1645 to 8.1027 mol dm^{-3}). The uppermost spectrum is that of pure water. It is evident from the spectra in Figure 2 that the OH stretch region has several component bands whose relative intensities change

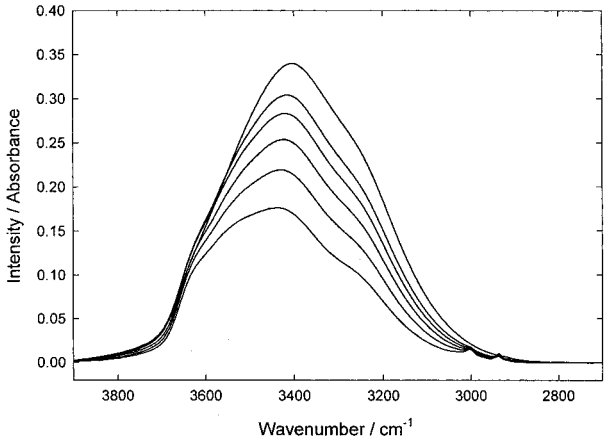

Figure 2. Selected examples of the IR spectra of water−EC mixtures in the 3900−2700 cm^{-1} region. Pure water is shown as the uppermost spectrum, the remaining spectra at lower intensity represent different mole ratios of water to EC (MR) and are, from top to bottom, 3.22, 5.30, 8.47, 12.58, and 19.87.

with changing water content. A systematic SVD survey of the OH stretch region from 3900 to 2700 cm^{-1} gave two distinctly different results. For high water content (MRs from 333.06 to 10.07 and pure water), there are two significant spectra that account for 99.999% of the variance. At lower water content (MRs from 8.47 to 3.22), there are three significant spectra that account for 99.999% of the variance. The inclusion of the small ν_{CH} bands of EC in the SVD survey did not significantly affect the results.

It is reasonable to assume that the number of significant abstract spectra determined from the SVD analysis is related to the number of significantly different environments in which water may be involved through different hydrogen-bonding arrangements. Because there is a clear division at 10.07 MR for the number of significant spectra, the discussion to follow has been divided into two sections, namely, one for high water content (MR > 10.07) and one for low water content (MR < 10.07).

Infrared spectra of a pure water solution collected at one temperature will be considered constant and termed the spectrum of "bulk" water. In water−EC solution mixtures, it is assumed here that water molecules not influenced by the presence of EC will have the same structure as pure water, as well as the same vibrational spectrum. The OH stretch vibrations of water molecules solvating EC are expected to have an infrared spectrum that is different than the infrared spectrum of bulk water. The solvating water molecules will be termed "bound" water. This description encompasses all water molecules that participate in the hydration of EC and includes water molecules in the first solvation shell, as well as water at progressively further distances from EC that does not have the structure of bulk water. At very high MRs, the observed infrared spectrum will predominantly reflect the infrared spectrum of bulk water with very little contribution from the spectrum of bound water, while at low MRs, the observed infrared spectrum will reflect the spectrum of bound water more so than that of bulk water.

If this hypothesis of bulk or bound water species is reasonable, then two physically real basis spectra[30] can be obtained from the two abstract spectra in the high-water-content solutions using factor analysis[37] and a user-defined model.[30,36] Eight infrared spectra with MRs from 10.07 to 333.06, including the spectrum of pure water, were used to create the raw data matrix **A** between 3900 and 2600 cm^{-1}. The following mathematical model was used to generate the matrix **P** that accounts for the contribution

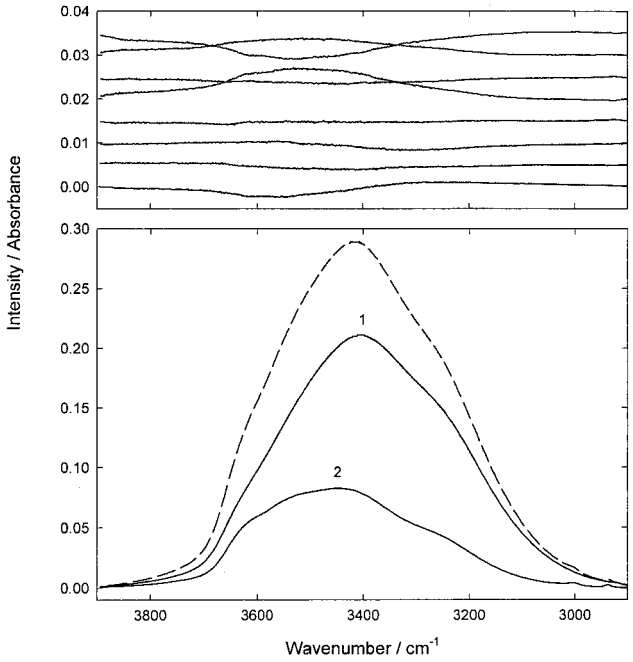

Figure 3. Factor analysis curve fits of the OH stretch region of water and EC based on the model described by eqs 2 and 3 and using the number of water molecules influenced by EC equal to 4. (Top) The residuals shown (offset for clarity) are from the curve fits from pure water and 333.06, 74.10, 21.64, 19.87, 16.17, 12.58, and 10.07 MR water−EC (from bottom to top). (Bottom) The curve fit of 16.17 MR water−EC solution. The dashed line indicates the measured spectrum. The numbers 1 and 2 on the graph indicate the spectra of bulk and bound water, respectively.

of each of the physically real basis spectra to each of the raw data spectra.[30]

$$P_{1j} = \frac{c_{H_2O_j} - nc_{EC_j}}{c_{H_2O_j} - nc_{EC_m}} \quad (2)$$

$$P_{2j} = \frac{c_{EC_j}}{c_{EC_m}} \quad (3)$$

In these equations, the subscript j is the jth column of **P**, n is the solvation number of EC, c_{Xj} is the concentration of species X (where X is water or EC) in the jth solution, and m indicates the highest concentration. Equation 2 models the integrated absorbance of bulk water, whereas eq 3 models the integrated absorbance of bound water. The model requires the solvation number for EC as a known parameter. However, n can be a fixed parameter, and curve fitting can be performed for a range of possible values of n.

The matrix elements P_{1j} and P_{2j} are the fractional contributions of the physically real basis spectra 1 and 2, respectively, to the jth raw data spectrum. P_{1j} is defined with respect the concentration of free water and corresponds to the spectral contribution of free water in the raw data spectrum of the solution containing the highest contribution of free water. Likewise, P_{2j} is defined with respect to the concentration of bound water in the solution containing the highest concentration of bound water. The highest concentration for water is that of pure water (55.3422 mol dm^{-3}), and for EC (bound water), the highest concentration was 4.0750 mol dm^{-3} (MR = 10.07). For this reason, one of the two physically real basis spectra should be identical to the spectrum of the pure solvent.

Figure 3 is a representative curve fit from the factor analysis

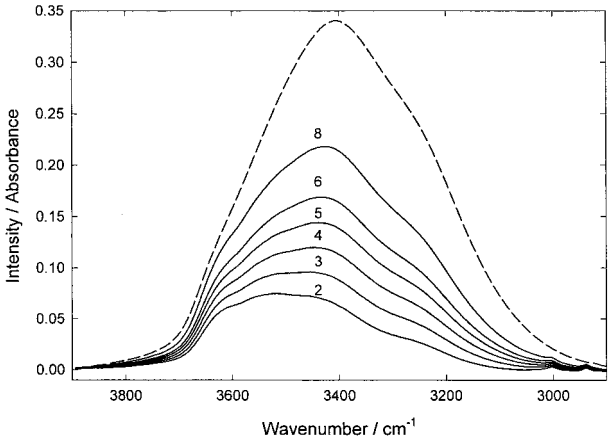

Figure 4. Water OH stretch spectral region of the physically real basis spectra accounting for EC association, for possible values of solvation number of 2, 3, 4, 5, 6, and 8 (labeled on the graph) The spectra are based on the model described by eqs 2 and 2. The physically real basis spectrum accounting for pure water is shown as a dashed line; the spectrum was obtained by factor analysis using $n = 4$.

of the solution with MR = 16.17 and assuming that $n = 4$. Also shown are the residuals for the curve fits of all eight spectra used to create the raw data matrix **A**. One of the two physically real basis spectra is identical to the spectrum of pure water and represents the fractional contribution to the infrared spectrum from bulk water. The second basis spectrum represents the spectrum of water that is bound to EC. The intensity distribution of the OH stretch component bands in the spectrum of bound water are more intense at higher wavenumbers compared to that from the spectrum of bulk water. This is in keeping with the general observation that water involved in decreased hydrogen-bonding environments has vibrational modes appearing at higher wavenumbers.[2] On the basis of the residual spectra shown in Figure 3 and a statistical measure of the goodness of fit (the sum of squares of deviations), the overall curve fits are excellent. Results such as those shown in Figure 3 are found for all integer values of n in the range 2−8.

Figure 4 shows all of the second physically real basis spectra, that is, the bound water spectra determined from the factor analysis for integer values of n from 2 to 8. Included in this figure is the first physically real basis spectrum, which is identical for all values of n, as well as the spectrum of pure water. The value of the solvation number used in eq 2 of the factor analysis significantly alters the appearance of the second basis spectrum. As n increases to 8, the second basis spectra approach the same shape as the first basis spectrum, although with the maximum intensity slightly displaced to a higher wavenumber. Alternatively, as n decreases to 2, two bands at high wavenumber begin to dominate the second basis spectrum. Neither the residual spectra nor the curve-fit spectra from the factor analysis are able to uniquely identify which value of n is appropriate.

The SVD analysis of the low-water-content solutions, MR from 10.07 to 3.22, identified three significant abstract spectra. Unfortunately, eqs 2 and 3 are now no longer valid, and a suitable model that describes the concentration changes of three types of water environments does not exist at this time. Even so, the fact that three abstract spectra were clearly identified in the low-MR range of solutions is itself an important result. Speculation as to the origin of these spectra can be made only in general terms and with respect to possible environments of water molecules. It is not known whether any of the abstract spectra are related to the spectrum of bulk water. The intensity distribution of the water OH stretch vibrations at high wavenumbers becomes dominant as the MR of the solutions shifts to lower values. A similar change in the intensity distribution is observed in ether−water[16,19] and acetonitrile−water mixtures[38] and is typically related to hydrogen-bonding changes.

3.2. Deconvolution of the *ν*OH Bands. Deconvolution of the OH stretch bands of water in water−solute mixtures is an alternative approach to factor analysis that can provide useful information concerning the relative amounts of different OH oscillators that are present. Although the procedure of decomposing spectral bands without any knowledge of the true number of composite bands can give misleading results,[2,39] there is still merit in attempting the deconvolution of the water OH stretch region.[19,39,40] Yarwood et al.[39] studied the structure of water molecules in polymeric matrixes by examining the deconvoluted OH stretch spectra of water sorbed into two polymer materials. The curve-fit spectra were used to monitor water sorption and desorption in the matrix as a function of time. The spectra demonstrated the time dependent changes in the strength of the hydrogen-bonded water network as the amount of water in the pores of the polymer changed.[39] Nickolov et al.[19] used the deconvolution method of band analysis to study the optimum hydration structure of water in two crown ether−water mixtures, 18C6 and 15C5. Their results were compared to Monte Carlo calculations and were found to agree well with the conclusions from computer simulations.[19]

Deconvolution of the OH stretch region of a water−solute solution mixture typically yields four or five component bands that are specifically related to the water OH stretch modes. Each of the component bands of water exhibit varying degrees of sensitivity toward changes in the hydrogen-bonding network. The relative changes to component band parameters such as area, width, and height over the range of water−solute mixtures examined can be correlated to changes in both the strength and the amount of hydrogen bonding.[19, 39]

Figure 5A and B presents examples of the decomposition of the OH stretch region of a pure water spectrum into five component bands. Also shown are the residual spectra that have been scaled by 10 and offset for clarity. Panels A and B of Figure 5 represent two separate curve fits that had different initial starting conditions. Both curve fits arrived at minima in their iterative calculations that were numerically (χ^2) similar, and their residual spectra are only marginally different from one another. Interestingly, the literature is not consistent regarding the relative intensities of the water component bands determined by deconvolution. Examples of both types of the curve fits shown in Figure 5A and B can be found among the range of systems examined. Figure 5A has component band ratios similar to the curve fits described by Nickolov et al.[19] for the crown ether−water solutions and by Dias et al.[40] for water−polymer membranes. On the other hand, Figure 5B has component band ratios more in keeping with curve fitting results from Yarwood et al. of pure water[39] and water−polymer matrixes.[39,41] However, all of the above-mentioned authors curve fit their ATR spectra without first correcting for spectral distortions.

It is not possbile to confidently constrain the component bands to a designated band shape during the curve fit. Because the trends are of value in this analysis, the curve fitting was performed for fixed band shapes. The deconvolving bands were constrained to band shapes determined from the best fit of pure water. They correspond to (Figure 5A) band shapes at 30, 0, 0, 5, and 100% Lorentzian (curve fit A) and (Figure 5B) band shapes set at 45, 0, 0, 0, and 100% Lorentzian (curve fit B) for

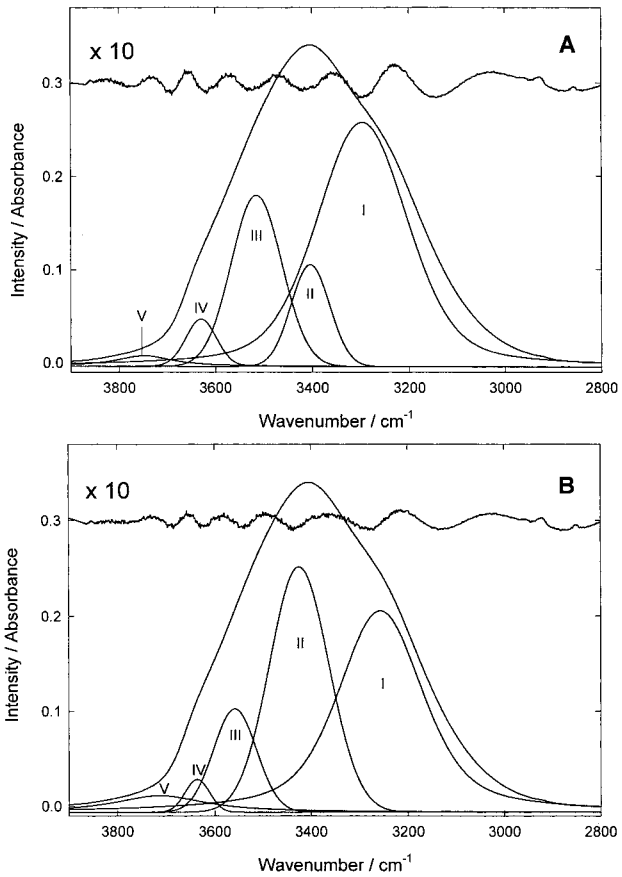

Figure 5. Five component bands deconvoluted from the infrared spectrum of pure water in the region 3900−2800 cm^{-1}. Panels A and B represent the best curve fits obtained from two different initial starting conditions (see text). The residual spectra are offset for clarity and are scaled by 10. Peak labels I to V refer to bands assignments given in the text.

components I, II, III, IV, and V, respectively. These two sets of band shape values were then fixed and used for all curve fitting routines over the range of water−EC solutions examined. All other peak parameters were allowed to vary during the iteration. Additionally, the ν_{CH} bands of EC were included to obtain a more accurate appraisal of component band I.

At this time, it is worth noting that several other methods of curve fitting were attempted to determine the best curve-fitting results. These included fixing all of the water deconvoluted bands at one band shape, as is commonly found in the literature, to either Gaussian or 20%, 30%, or 40% Lorentzian. The results of these curve fits are not given here because the curve fitting was not as satisfactory as the mixed band shapes described earlier. Also, a significantly improved curve fit was attained with the inclusion of a fifth component band (V) at higher wavenumbers. This is not a desirable addition because the additional degree of freedom in the curve fitting procedure always produces a better curve fit. Moreover, the curve fit of component V was found to be extremely variable, and it is likely that this peak is not genuine but is, in fact, due to some nonlinear feature of the baseline.

The residual spectra shown in panels A and B of Figure 5 show the curve fit is not as good at lower wavenumbers as it is at higher wavenumbers. The reason for this is not known but is likely related to the baseline subtraction procedure. Incorporation of an additional band into the curve fit to account for the poorer fit in this region could not be justified.

The interpretation of the deconvoluted component bands must take into account that the bands represent water in all possible

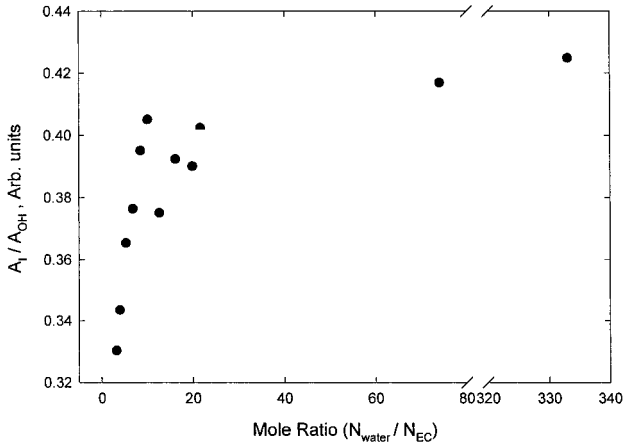

Figure 6. Plot of the relative area, A_I/A_{OH}, for the normalized[42] OH stretch deconvoluted component band I against the MR and using the band shapes described in the text as curve fit B.

environments, bound and bulk, and that the relative significance of these environments is changing as the MR is altered. Accordingly, the vibrational assignments of the deconvoluted bands must reflect this change. At higher water content (MR > 10), the area of each deconvoluted component band will be dominated by the contribution from water in the bulk phase with smaller contributions from bound water. At higher EC concentrations (MR < 10), the deconvoluted OH bands of water will most likely be dominated by EC interactions.

An appropriate choice of band shape parameters with which to deconvolute the νOH bands of water from the normalized infrared spectra of water−EC solutions was chosen. The decision to use only the band shape parameters from curve fit B is based upon two observations, namely, the value of χ^2 and the residual spectra obtained from the curve fits. These results are in favor of curve fit B over all other band shape parameters examined during the deconvolutions. The component band trends for the relative (normalized[42]) band areas for bands I, II, III, and IV were examined following a procedure used by Nickolov et al.[19] Because the plots determined by this method were markedly similar to the results of Nickolov, all of the graphs will not be shown. Instead, only the results for component band I are given, Figure 6, while Table 1 shows the results for all four bands.

In pure liquid water, component bands I and II are assigned to fully hydrogen-bonded water molecules, such that band I is the ν_s OH stretch for tetrahedrally coordinated water and band II is the ν_{as} OH for water that is not fully coordinated. The two highest-wavenumber component bands are assigned OH stretch modes of water molecules that are not fully (partially or unsymmetrically) hydrogen-bonded. The unsymmetrical bonding of the water molecule is represented here by H^f-O−H^b such that the OH^b oscillator is hydrogen-bonded to another molecule, while the OH^f oscillator is free (or weakly hydrogen-bonded). Band III is assigned to be the νOH^b stretch mode, and band IV is assigned to νOH^f stretch mode.

At MR > 20, the slope of the graph is relatively linear and shallow compared to the slope of the graph at lower MRs. This is expected because the high water content of these solutions will give deconvoluted bands with A_I/A_{OH} ratios similar to those of pure water. The contribution to the curve fit from bound water will likely be swamped by the contribution due to bulk water. As the MR approaches 20, the water−water bonds are increasingly broken and replaced with water−EC bonds, and the slopes of the graphs tend away from their shallow linearity. For 20 > MR > 10, the normalized infrared spectra of the OH stretch

TABLE 1: Results of Curve Fit B[a] for Mole Ratio Changes to the Water−EC Mixture

mole ratio	position (cm^{-1})	area	width (cm^{-1})	position (cm^{-1})	area	width (cm^{-1})
	Component Band I			Component Band II		
333.05	3250	0.437	225	3418	0.396	176
74.09	3250	0.429	223	3420	0.406	176
21.64	3253	0.417	219	3424	0.411	174
19.87	3254	0.414	219	3425	0.378	174
16.16	3254	0.409	217	3426	0.419	174
12.58	3255	0.400	215	3428	0.422	173
10.06	3265	0.423	218	3435	0.403	167
8.46	3265	0.415	217	3436	0.410	168
6.81	3261	0.394	213	3434	0.422	170
5.29	3263	0.380	210	3437	0.430	170
3.96	3261	0.358	206	3437	0.439	171
3.21	3262	0.342	202	3439	0.445	171
	Component Band III			Component Band IV		
333.05	3559	0.152	143	3637	0.014	66
74.09	3562	0.150	140	3637	0.015	65
21.64	3562	0.152	132	3635	0.020	64
19.87	3563	0.140	132	3635	0.017	62
16.16	3563	0.150	129	3635	0.022	64
12.58	3564	0.157	129	3634	0.021	62
10.06	3564	0.143	117	3635	0.030	65
8.46	3566	0.146	117	3635	0.029	62
6.81	3566	0.153	117	3635	0.031	63
5.29	3569	0.160	118	3636	0.030	60
3.96	3571	0.172	119	3636	0.031	59
3.21	3573	0.182	119	3637	0.031	57

[a] Refer to text. [b] Infrared spectra are normalized[42] to EC.

bands will have contributions from two sources, bulk and bound water species. The OH deconvoluted bands determined from the curve fit of these solutions represent an average OH environment summed over both the bulk and the bound water molecules.

At MR < 10, the plot of relative integrated area against MR has a continuous steep decrease for the case of A_I/A_{OH} (and continuous steep increases for A_{II}/A_{OH}, A_{III}/A_{OH}, and A_{IV}/A_{OH}). The trend for component band I indicates that the strong and uniform hydrogen bonding in solution is rapidly decreasing. However, component band I is clearly present even at the lowest-MR solutions examined. If this band is attributed to bulk water only, then two assumptions can be made. Either solution heterogeneity exists even at the lowest MR, or some water molecules are fully hydrogen-bonded to EC (or to neighboring water molecules) in orientations that give rise to symmetric OH stretch motions. The perturbation of this OH oscillator will be discussed further in section 3.3.

Using the results such as those shown in Figure 6, Nickolov deduced the optimum hydration number for water and crown ether solutions. However, EC is not expected to rigidly bind water molecules in the same way as the crown ether molecules. Therefore, the apparent value of approximately 10 as the optimum hydration number for EC, determined from the change of the slope in Figure 6, is intuitively too high. Alternatively, the determination of the number of induced structural defects of bulk water when EC is added was conducted using a method described in section 3.3.

3.3. Perturbation of the ν_{sym}OH Mode (Band I) of Water. A factor that also contributes to the intensity profile changes of an infrared band is the change in the molar absorption coefficient when a molecule participates in association mechanisms. Water molecules that have been perturbed by changing their hydrogen-bonding environment away from that of bulk water to those that are bound to EC will cause a change to the molar absorption coefficient of the absorption band. The magnitude of the molar absorption coefficient change in the intensity profile of the deconvoluted band (measured as the integrated band area) is not known. However, such changes have been approximated for the case of water adsorbed into polymer matrixes.[39] The well-known relationship relating absorbance to molar absorption coefficient is given in eq 4

$$A = \log\left(\frac{I_0}{I}\right)_\nu = \epsilon_\nu cl \tag{4}$$

where A is the absorbance of a band at wavenumber ν, ϵ is the molar absorption coefficient, c is the concentration, and l is the path length of the infrared light through the solution (equal to 1.00 μm). Following Yarwood et al.,[39] the integrated band intensity, I_c, measured as band area is given by eq 5.

$$C = \int \epsilon_\nu \, d\nu = \text{area}/cl \tag{5}$$

The value of ϵ, and therefore C, is known to depend on the perturbation of the molecular environment.[39] By comparing the C values for water in specific environments to that of pure water, water as ice, or a hypothetical value for full hydrogen bonding, some measure of the OH oscillator perturbation due to association can be made. Maeda and Kitano[23] have reviewed this approach to the analysis of the collective symmetric stretch mode of water (component band I), determined from the Raman spectra of water solutions. Studies[6,23−25,39] of the deconvoluted Raman spectra using the collective mode analysis have offered a means by which one can compare different solutes in water and their effect on the hydrogen-bonding network.

The collective mode band intensity, I_c, of the symmetric OH vibration is known[6,23−25] to arise from the structure of the tetrahedral water network. Ice that has the structure I_h is defect-free, that is, all of the OH oscillators are fully tetrahedrally bonded. Decoupling of the OH oscillators because of defects arising from the destruction of this tetrahedral network, such as a reduced coordination number from fewer nearest neighbors, will lead to a decrease in the collective intensity of the mode. For pure liquid water, the value of C [$C_w(T)$] reduces linearly with an increase in temperature because of hydrogen-bond defects, such that

$$C_w(T) = C_{ice}(1 - p_1)^2 \tag{6}$$

where p_I is the probability that an OH oscillator has a vibrational defect and C_{ice} is the C value for the defect-free reference network of ice ($C_{ice} = 0.54$).[23] Water molecules that are restricted in their orientation in the hydration shell of solutes will further reduce the value of C [$C_x(T)$].

The probability, P_d, that an OH oscillator is excluded from the hydrogen-bonding network of water molecules because of its position and orientation with respect to solutes is defined as[23]

$$P_d = \frac{C_w(T) - C_x(T)}{C_w(T)} \tag{7}$$

Hence

$$C_x = C_w(T)(1 - P_d) = C_x(1 - p_1)^2 \tag{8}$$

The hypothetical value for C for a fully hydrogen-bonded reference network containing the solute is given as C_x [which equals $C_{ice}(1 - P_d)$].[23] Defining the number of defects per EC molecule as N, which corresponds to the number of OH

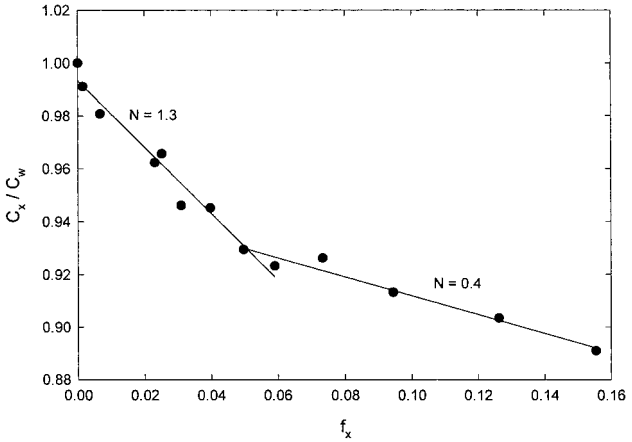

Figure 7. Ratio of the collective band area (for component band I) of the sample to that of pure water, C_x/C_w, plotted against f_x, the ratio of EC molecules to the number of OH oscillators in solution at 24 °C.

oscillators excluded from the tetrahedral network,[23,25] N is given by eq 9, where f_x is the number of EC molecules per OH oscillator.

$$N = \frac{P_d}{f_x} \tag{9}$$

A comparison of the C values for water−EC solutions with those for pure liquid water (C_x/C_w) plotted against f_x should allow a reasonable estimate of the perturbation. A value of C_x smaller than that of pure water at the same temperature, C_w, such that $C_x/C_w < 1$ indicates the breakdown of water−water hydrogen bonds. Conversely, if $C_x/C_w > 1$, then the addition of a solute has enhanced the water−water hydrogen-bond structure. A comparison has been made for water−EC solutions and is shown in Figure 7. The correlation of C_x/C_w to f_x is clearly demonstrated in which the values of C_x/C_w were determined from the area of component band I using eq 5.

Two features of Figure 7 are noteworthy. First, the addition of EC disrupts the hydrogen bonding of water, as evidenced by the values of C_x/C_w being less than 1. Also, a continuous increase in the EC content of the solutions further decreases the values of C_x/C_w. Second, there is clearly a discontinuous section to the plot of C_x/C_w against f_x that occurs at $f_x \approx 0.5$ (MR $\approx$ 10). Such changes to the slope are similarly observed in polymer solutions and have been interpreted in terms of structural changes in the polymer.

At MR > 10 ($f_x < 0.05$), one EC molecule induces 1.3 defects in the water network, and in the region where MR < 10 ($f_x > 0.05$), the number of defects decreases to 0.4. Kitano et al.[25] observed similar trends for the value of N determined from the Raman spectra of polymer gels in water. As the concentration of the polymer gel in water increases to a critical point, the polymer chains entangle each other to make a pseudo network; once this occurs, the value for N was found to decrease. Thus, macroscopic changes in the polymer gel structure induce structural changes in the water network. Kitano et al.[26] more recently suggested that water in both polymer solutions and gels could be divided into three components, (a) hydration water, (b) water in spaces surrounded by the polymer (*interstitial water*), and (c) bulk water.

The N values for linear polymers, at low concentration, largely depend on the properties of the monomer units of the polymer gel.[25] A list of some selected N values for monomer units of polymer solutions has been compiled,[23] and the trends are indicative of the degree of hydrophobicity of the units. Ionisable groups and counterions have larger values of N than neutral polymers. Of the neutral polymers, the hydrophobicity of functional group moieties and side chains also play a role in the value of N; thus, the less polar the group, the lower the value of N.

The value of N (0.4) compared to previously compiled data[23] is lower than values found for relatively hydrophobic groups and side chains. An important point to be noted here is that the choice of curve fitting method was found to significantly affect the absolute values of N; however, the trends in these plots were the same. A possible conclusion that relates the slope changes can be envisioned by a relationship between the solvent-accessable sites of EC. The self-association of EC molecules as dimers or higher-order polymers involves the carbonyl oxygen and possibly the ring oxygens. Hence, the self-association of EC decreases the availability of sites for water to hydrogen bond, thereby increasing the hydrophobic nature of the solvent−solute interaction. Thus, the structure of the EC molecules in solution relative to one another is changing significantly for $f_x > 0.05$, which corresponds to MR < 10.

The number of defects per EC, N, should correspond to the mean number of solvating water molecules, that is, the value of n determined from factor analysis. As previously mentioned, the absolute value of N was dependent upon the user-defined curve fitting parameters. However, the independently obtained results from factor analysis and perturbation of the OH oscillator have unambiguously identified a narrow range over which the structure of the solute−solvent solution changes significantly for water−EC solutions with a maximum EC content of 60 mass %; that change occurs at MR $\approx$ 10.

3.4. Component Band Positions and Widths. Table 1 shows the behavior of the component band positions and bandwidths from the curve fit of the normalized spectra. The frequency of the OH oscillator is strongly correlated to the O−H···O hydrogen-bond distance between the hydrogen atom of the OH group and the oxygen atom of a neighboring molecule.[8] Component band I has a sharp maximum at MR $\approx$ 10; bands II and III show an increase in wavenumber as the water content decreases but no well-defined minimum or maximum. Band IV has a well-expressed minimum at MR $\approx$ 15.

Hydrogen bonding causes the OH stretch vibrations of water to shift to lower wavenumbers.[21] On this premise, the shift to (generally) higher wavenumber for component bands II, III, and IV indicates a decrease in the strength of the hydrogen bonding. Component band I has a maximum at MR = 10, while at values on either side of MR = 10, the hydrogen bonding is increased. Nickolov et al.[19] have observed the same phenomena with crown ether−water solutions and postulated that it represents a shortening of the OH···O bond distance between water species. This can be rationalized by water existing in largely hydrophobic environments as the EC content in the solution becomes high.

Additionally, the bandwidths of all four component bands gradually decrease as MR goes from 20 to 3.22; for MR > 20 the bandwidths remained reasonable constant. The bandwidths of the deconvoluted bands are correlated with the variety of hydrogen bonds of each kind. A decrease in component bandwidth is indicative of water having fewer degrees of freedom as a result of the formation of a range of bond lengths and bond angles.

4. Conclusions

The analyses of the infrared vibration modes of water in mixed EC−water solutions using the results of factor analysis and curve-fitting routines have been compared with an emphasis

on the limitations of each technique. The SVD results are invaluable in that a specific number of basis spectra can be unambiguously identified. The failure of the factor analysis lies in the inability of the user to provide a suitable model for describing the solution changes once the number of significant basis spectra exceeds two. Curve fitting of the OH stretching vibrational envelope of water into four decomposed component bands and subsequent interpretation of the band parameters are somewhat subjective and depend on the choice of parameters used for the curve-fitting routine. However, it is reasonable to interpret the deconvoluted band parameters of the curve fit in terms of relative changes that occur in the structure of water upon addition of EC to the solution.

The results from the SVD and the curve fitting provide evidence for significant structural changes to the water−EC solutions as the MR decreases. The association of EC molecules into a pseudo network at low MR is postulated as the principal factor determining the environment for water molecules. A critical MR value of approximately 10 was found to be the point at which the water−EC solution structure significantly changes. MR values lower than 10 were postulated to have little water remaining as bulk water so that the principal influence upon the remaining bulk water was from hydrophobic interactions with EC.

Acknowledgment. P.A.B. thanks Dr. John Loring for the use of his curve-fitting programs and the many useful discussions concerning the optics and strategies for ATR infrared spectroscopy. The authors gratefully acknowledge financial support from the National Science Foundation, Washington, D.C. (CHE-9729314).

References and Notes

(1) Mirabella, Francis M., Ed. *Internal Reflection Spectroscopy. Theory and Applications;* Practical Spectroscopy Series.; Marcel Dekker Inc.: New York, 1993; Vol. 15.

(2) Libnau, F. O.; Toft, J.; Christy, A. A.; Kvalheim, O. M. *J. Am. Chem. Soc.* **1994**, *116*, 8311.

(3) Carey, D. M.; Korenowski, G. M. *J. Chem. Phys.* **1998**, *108*, 2669.

(4) Marechal, Y. *J. Mol. Struct.* **1994**, *322*, 105.

(5) Marechal, Y. *J. Phys. Chem.* **1993**, *97*, 2846.

(6) Green, J. L.; Lacey, A. R.; Sceats, M. G. *J. Phys. Chem.* **1986**, *90*, 3958.

(7) Hare, D. E.; Sorensen, C. M. *J. Chem. Phys.* **1992**, *96*, 13.

(8) Nienhuys, H.-K.; Woutersen, S.; van Santen, R. A.; Bakker, H. J. *J. Chem. Phys.* **1999**, *111*, 1494.

(9) Luck, W. A. P.; Wess, T. *Can. J. Chem.* **1991**, *69*, 1819.

(10) Wall, T. T.; Hornig, D. F. *J. Chem. Phys.* **1965**, *43*, 2079.

(11) Glew, D. N.; Rath, N. S. *Can. J. Chem.* **1971**, *49*, 837.

(12) Stangret, J.; Gampe, T. *J. Phys. Chem. B* **1999**, *103*, 3778.

(13) Stangret, J.; Kamienska-Piotrowicz, E. *J. Chem. Soc., Faraday Trans.* **1997**, *93*, 3463.

(14) Bergstrom, P.-A.; Lindgren, J.; Kristiansson, O. *J. Phys. Chem.* **1991**, *95*, 8576.

(15) Kristiansson, O.; Eriksson, A.; Lindgren, J. *Acta Chem. Scand. A.* **1984**, *38*, 613.

(16) Hey, M. J.; Jackson, D. P. *Chem. Phys. Lett.* **1999**, *309*, 69.

(17) Goutev, N.; Nickolov, Z. S.; Matsuura, H. *J. Mol. Liq.* **1998**, *76*, 117.

(18) Goutev, N.; Nickolov, Z. S.; Georgiev, G.; Matsuura, H. *J. Chem. Soc., Faraday Trans.* **1997**, *93*, 3167.

(19) Nickolov, Z. S.; Ohno, K.; Matsuura, H. *J. Phys. Chem. A* **1999**, *103*, 7544.

(20) Bryan, S. A.; Willis, R. R.; Moyer, B. A. *J. Phys. Chem.* **1990**, *94*, 5230.

(21) Fischer, W. B.; Eysel, H.-H. *J. Mol. Struct.* **1997**, *415*, 249.

(22) Hecht, D.; Tadesse, L.; Walters, L. *J. Am. Chem. Soc.* **1993**, *115*, 3336.

(23) Maeda, Y.; Kitano, H. *Spectrochim. Acta A* **1995**, *51*, 2433.

(24) Green, J. L.; Lacey, A. R.; Sceats, M. G. *Chem. Phys. Lett.* **1987**, *134*, 385.

(25) Terada, T.; Maeda, Y.; Kitano, H. *J. Phys. Chem.* **1993**, *97*, 3619.

(26) Tsukida, N.; Muranaka, H.; Ide, M.; Maeda, Y.; Kitano, H. *J. Phys. Chem. B* **1997**, *101*, 6676.

(27) David Linden, Ed. *Handbook of Batteries.* 2nd ed.; McGraw-Hill: New York, 1994.

(28) Srivastava, A. K.; Samant, R. A.; Patankar, S. D. *J. Chem. Eng. Data* **1996**, *41*, 431.

(29) Loring, J. S. *Spectral Conversion Tool*; Department of Chemistry, UC Davis, 1998−1999.

(30) Loring, J. S.; Fawcett, W. R. *J. Phys. Chem. A* **1999**, *103*, 3608.

(31) Sperline, R. P.; Muralidharan, S.; Freiser, H. *Appl. Spectrosc.* **1986**, *40*, 1019.

(32) Bertie, J. E.; Zhang, S. L.; Jones, R. N.; Apelbat, Y.; Keefe, C. D. *Appl. Spectrosc.* **1995**, *49*, 1821.

(33) Bertie, J. E. *Appl. Spectrosc.* **1985**, *39*, 392.

(34) Bertie, J. E.; Zhang, S. L.; Manji, R. *Appl. Spectrosc.* **1992**, *46*, 1660.

(35) Loring, J. S. *LinkFit*; Department of Chemistry, UC Davis, 1996−1999.

(36) Loring, J. S. *SVD Spectral Analysis Tool*; Department of Chemistry, UC Davis, 1997−1999.

(37) Malinowski, E. R. *Factor Analysis in Chemistry*, 2nd ed.; John Wiley and Sons: New York, 1991.

(38) Bertie, J. E.; Lan, Z. *J. Phys. Chem. B* **1997**, *101*, 4111.

(39) Sammon, C.; Mura, C.; Yarwood, J.; Everall, N.; Swart, R.; Hodge, D. *J. Phys. Chem. B* **1998**, *102*, 3402.

(40) Dias, C. R.; Norberta de Pinho, M. *J. Mol. Liq.* **1999**, *80*, 117.

(41) Yarwood, J.; Mura, C.; Sammon, C.; Pereira, M. *J. Mol. Liq.* **1999**, *80*, 93.

(42) Using the method in ref 19, the water OH bands were normalized to the area of an EC band appearing at 1483 cm^{-1} (ν_3, CH_2 scissor). The ν_3 vibration is considered the best candidate for which to normalize the infrared spectra because the band center does not shift by more than 1 cm^{-1} and the peak area follows the linear slope expected from the Beer−Lambert equation for all EC concentrations used in the analysis. Every spectrum was normalized to the area of its ν_3 band, and the area was determined from a curve fit of the band after baseline correction. It is necessary to curve fit the band because a weak absorption appears on the high-wavenumber side of ν_3 at high EC concentration. Normalization of the spectra correctly gave a linear plot of mole ratio (N_{water}/N_{EC}) and of the total integrated area of the ν_{OH} band (A_{OH}). The small ν_{CH} stretch bands at 3002 and 2937 cm^{-1} account for less than 1% of the total band envelope at the lowest mole ratio, and their contribution was not removed from the data.